ELSEVIER

European Journal of Pharmacology 316 (1996) 87–95

ejp

The local anesthetic, *n*-butyl-*p*-aminobenzoate, reduces rat sensory neuron excitability by differential actions on fast and slow Na^+ current components

Rutgeris J. Van den Berg [a,*], Zheng Wang [a], Rene J.E. Grouls [b], Hendrikus H.M. Korsten [b,c]

[a] *Department of Physiology and Physiological Physics, Laboratory of Physiology, University of Leiden, Wassenaarseweg 62, PO Box 9604, 2300 RC Leiden, The Netherlands*

[b] *Department of Pharmaceutical Services, Catharina Hospital, Eindhoven, The Netherlands*

[c] *Department of Anesthesiology, Catharina Hospital, Eindhoven, The Netherlands*

Received 1 February 1996; revised 6 August 1996; accepted 9 August 1996

Abstract

Effects of the local anesthetic, *n*-butyl-*p*-aminobenzoate, at a concentration of 100 μM, were investigated using the whole-cell voltage clamp on dorsal root ganglion neurons cultured from neonatal rat in a serum-enriched medium. During current clamp conditions, the drug either increased the firing threshold or blocked tetrodotoxin-sensitive and tetrodotoxin-resistant Na^+ action potentials. These actions were reversible. Under voltage clamp conditions, inactivation of the Na^+ current revealed the existence of 3 fast Na^+ current components, termed F_1, F_2 and F_3 (tetrodotoxin-sensitive) and 2 slow ones, termed S_1 and S_2 (tetrodotoxin-resistant). The local anesthetic shifted the midpoint potentials of Na^+ inactivation curves for F_1, F_2 and F_3 currents by 7, 21 and 6 mV, respectively, towards hyperpolarizing membrane voltages whereas it did not influence these potentials for the slow currents. The amplitudes of only F_3 and S_2 currents were reduced by *n*-butyl-*p*-aminobenzoate to 24 and 11%, respectively, of their control values. These results show that the local anesthetic has a differential mode of action on the 5 types of Na^+ currents, which are apparently present in cultured sensory neurons. This differential action can play an important role in the selective analgesic effect observed after epidural administration of a 10% *n*-butyl-*p*-aminobenzoate suspension.

Keywords: Local anesthetic; *N*-butyl-*p*-aminobenzoate; Patch clamp; Na^+ current inactivation; Dorsal root ganglion

1. Introduction

Long-lasting relief of intractable pain in terminal cancer patients was successfully achieved by Shulman (1987), who used epidural injection of an aqueous suspension of *n*-butyl-*p*-aminobenzoate. Surprisingly, no signs of reduced motor functions were observed. We obtained similar results using *n*-butyl-*p*-aminobenzoate particle suspensions in a solvent consisting of physiological saline and the surfactant polysorbate 80 (Korsten et al., 1991). Thus, the epidural application of such suspensions is a promising approach for the relief of severe chronic pain. It is unknown whether the effect of this treatment originates from the suspension, the dissolved local anesthetic, the surfactant or the specific site of application. Previously, we tested the action of the dissolved drug on the Na^+ current in neonatal dorsal root ganglion neurons, cultured in a chemically defined, serum-free medium. In these experiments, the Na^+ current consisted of a single fast and slow component (cf., Roy and Narahashi, 1992) and the local anesthetic shifted the inactivation curve of the fast current towards hyperpolarizing membrane voltages whereas the inactivation of the slow component was unaffected (Van den Berg et al., 1995a). On the other hand, dorsal root ganglion neurons cultured in serum-containing media exhibit multiple fast and slow Na^+ current components (Schwartz et al., 1990; Caffrey et al., 1992; Van den Berg et al., 1995b).

In the current study, we addressed the question of whether dissolved *n*-butyl-*p*-aminobenzoate could have a differential effect on the different types of fast and slow Na^+ currents. To this end, the patch-clamp technique was

* Corresponding author. Tel.: (31-71) 527-6812; Fax: (31-71) 527-6782.

PII S0014-2999(96)00638-3

applied to isolated small dorsal root ganglion neurons from the rat. These small-diameter neurons are probably the somata of slowly conducting myelinated A δ- and unmyelinated C-type neurons (Harper and Lawson, 1985), which include fibres that mediate pain (Baccaglini and Hogan, 1983). We found that the local anesthetic had a differential action on the fast and slow Na^+ current components, we had measured. The increase of the firing threshold and the block of action potentials in dorsal root ganglion neurons by the drug originated from the loss of available fast and slow Na^+ channels by either increased inactivation or channel block, which explains the analgesic action of the local anesthetic administered as a suspension to patients.

2. Materials and methods

The materials and methods used in this study have been described by Van den Berg et al. (1995a). Briefly, dorsal root ganglion neurons were cultured in F14 medium (Imperial Lab) enriched with 10% horse serum (Gibco; Wood et al., 1988) and patch-clamp measurements (Hamill et al., 1981) were performed on small-diameter neurons (10–15 μm) without processes, using the EPC-7 amplifier (List). Under current clamp conditions, the firing threshold was determined (Wang et al., 1994) and action potentials were recorded either every 6 s for 2 min or every 30 s for 5 min to follow the onset of and recovery from the local anesthetic effect. Under voltage clamp conditions (holding voltage V_H of −70 mV), voltage protocols were applied to measure the Na^+ current as a function of voltage and time and to obtain its inactivation properties (bandwidth 10 kHz). To evaluate the speed of the voltage clamp, the membrane current was measured in response to a hyperpolarizing voltage pulse in a wide frequency band (low-pass filter cut-off frequency 50 kHz), after compensation of the fast capacitative current. Averaging 25–36 (noisy) current traces yielded $< I_m(t) >$, which was fitted according to:

$$< I_m(t) > = I_c(O) e^{-t/\tau} + \Delta I_L \quad (1)$$

where $I_c(0)$ is the instantaneous uncompensated (slow) capacitative current arising from the series resistance and membrane capacitance, τ the decay time constant determining the speed of the voltage clamp and ΔI_L the change in the leakage current. The value of τ amounted to 159 ± 26 μs ($n = 23$) and was reduced by series resistance compensation by 50–85%, resulting in a critically damped response with a compensated time constant, $\tau_c < 100$ μs. The magnitudes of membrane resistance, series resistance and membrane capacitance were derived from Eqn. 1 (cf., Van den Berg et al., 1993), yielding 610 ± 80 MΩ (n = 22), 6.7 ± 0.7 MΩ and 23 ± 3 pF ($n = 23$), respectively.

The composition of the extracellular control solutions and of the pipette (intracellular) solutions is given in Table 1. Ca^{2+}-free solutions were used to measure exclusively Na^+ action potentials and Na^+ currents. A second and third type of extracellular solution had a composition similar to that of the control, but contained 100 μM *n*-butyl-*p*-aminobenzoate and 200 nM of the fast Na^+ channel blocker tetrodotoxin, respectively. To pharmacologically isolate Na^+ currents, the pipettes contained different K^+ channel blockers (cf., Omri and Meiri, 1990). ATP, tetrodotoxin and glucose were freshly added to the solutions. The pH of all solutions was adjusted to 7.4 immediately before use. The dish (≈ 0.5 ml) containing the neurons was continuously perfused at 2 ml/min with oxygenated extracellular solution. Incubation time with the drug was ≤ 5 min so that its effect would be reversible within 10 min (Van den Berg et al., 1995a). All experiments were done at room temperature (20 ± 1°C).

Special customized software (Biomav) was used to digitally correct the Na^+ currents for contributions of seal currents, residual capacity currents and membrane leakage currents. During voltage clamping, readjustments of capacitance and series resistance compensations were performed, after changing the extracellular solutions and before running the different voltage protocols. Curve-fitting was performed using the graphics program FigP6.0 (Biosoft) and FitBio (Biomav). For statistical evaluation the paired *t*-test was applied, using Asystant 1.1 (Asyst Software Technologies), with the level of significance (P) chosen as 0.05. The data are given as means ± S.E.M. with n as the number of neurons investigated.

3. Results

3.1. Tetrodotoxin-resistant and tetrodotoxin-sensitive action potentials

The firing of Na^+ action potentials was investigated in the absence and presence of 100 μM *n*-butyl-*p*-aminobenzoate, while the effect of the fast Na^+ channel blocker, tetrodotoxin (200 nM), was studied directly after wash-out

Table 1
Composition of the Ca^{2+}-free extra- and intracellular solutions (in mM)

	Current clamp		Voltage clamp	
	ECS	ICS	ECS	ICS
NaCl	130	8	130	8
KCl	5	140	–	–
CsCl	–	–	–	120
CsOH	–	–	5	15
TEA-Cl	–	–	10	5
4-AP	–	–	1	–
$MgSO_4 \cdot 7H_2O$	2.50	2.50	2.50	2.50
Choline-Cl	10	–	–	–
Hepes	10	10	10	10
EGTA	–	5	–	5
Na_2ATP	–	2	–	2
Glucose	10	10	10	10

ECS and ICS, extra- and intracellular solutions, respectively.

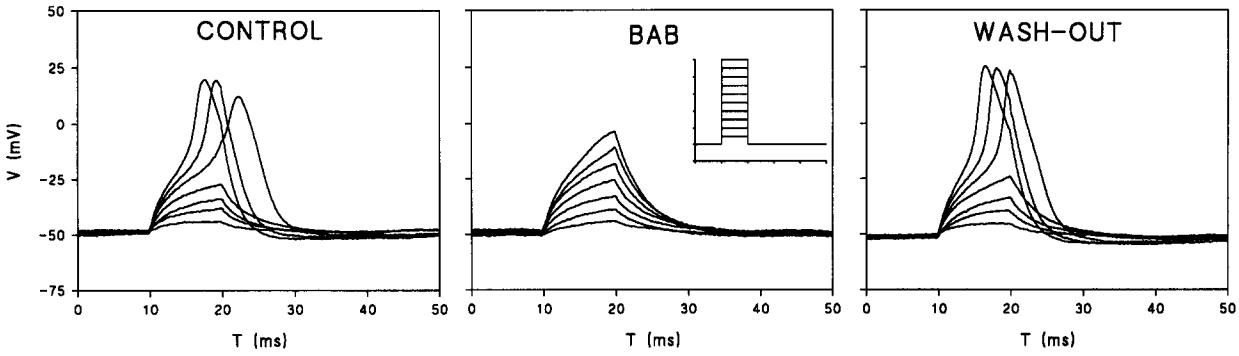

Fig. 1. Whole-cell current-clamp recordings in the absence and presence of the local anesthetic. *n*-Butyl-*p*-aminobenzoate-sensitive Na^+ action potentials of a dorsal root ganglion neuron with a resting membrane potential of −50 mV. Inset middle panel: current protocol applied. Current pulses differ by 20 pA. The first 3 subthreshold responses were not shown. Left panel: voltage responses in control solution. The threshold voltage was −18 mV. Middle panel: responses in the presence of the local anesthetic applied for about 2 min. The action potential started to fail after 26 s of incubation with the drug. Right panel: voltage responses recorded 5 min after the start of the wash-out. The magnitude of the firing threshold amounted to −20 mV. Action potentials re-appeared for the first time 46 s after replacement with control solution. During longer-lasting perfusions, the recovery from local anesthetic effect was longer (Van den Berg et al., 1995a). The action potential was tetrodotoxin-resistant.

of the local anesthetic. As is shown in Fig. 1, in 25 of 40 neurons the action potential was reversibly blocked by the local anesthetic. In 16 of these 25 neurons, the action potential could not be blocked by tetrodotoxin. Their threshold voltages, -22 ± 2 mV before tetrodotoxin perfusion, -20 ± 2 mV during tetrodotoxin application and

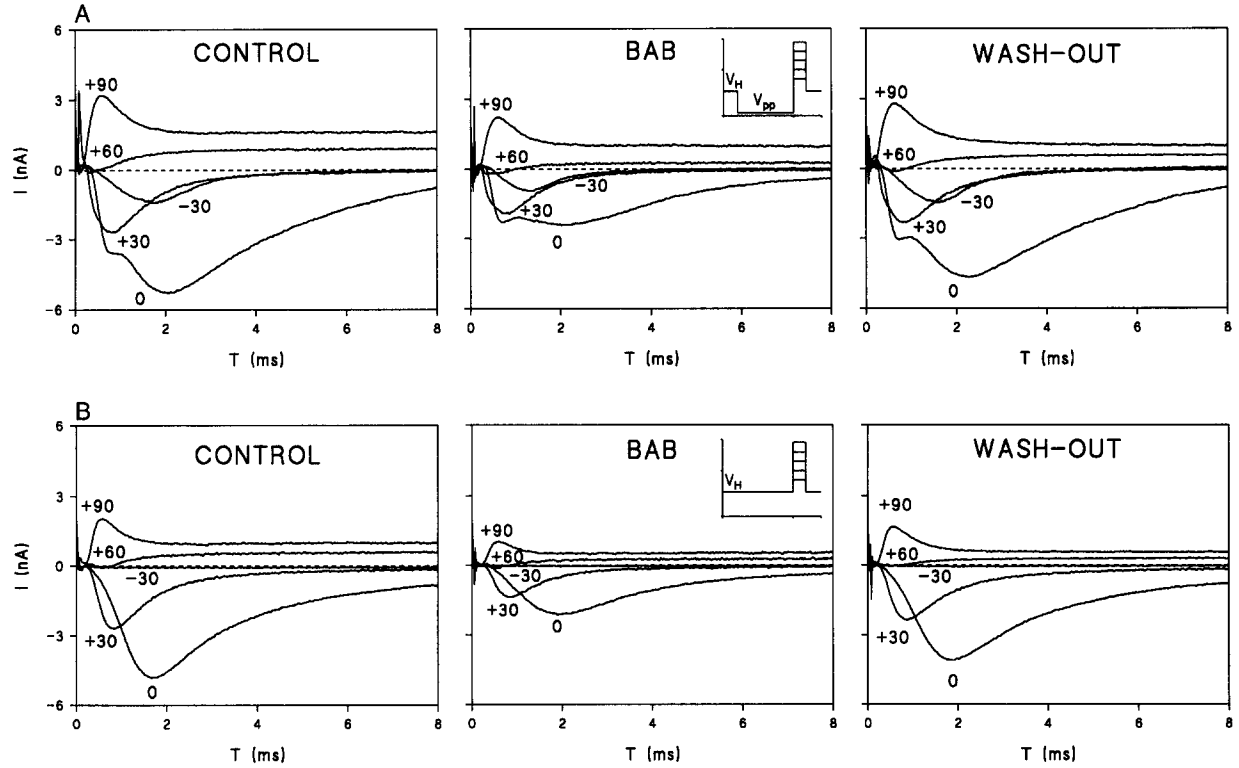

Fig. 2. Whole-cell voltage-clamp recordings in the absence and presence of the local anesthetic. For clarity, only 5 current traces out of 21 recordings are shown. Inset middle panel: activation protocol. The neuron had a capacitance of 16 pF and a resting membrane resistance of 500 MΩ. The series resistance (5 MΩ) was compensated by 50% and the (compensated) time constant of the capacity current amounted to 40 μs. (A) Na^+ currents, measured in response to different test potentials, as indicated, preceded by conditioning pre-pulse. Left panel: control currents. The fast current, dominating at −30 mV, activated within 500 μs and inactivated within a few ms. At 0 mV, the slow current activated within about 2 ms and inactivated slowly (> 10 ms). Middle panel: currents after 4-min perfusion with the local anesthetic. Right panel: currents after wash-out of the drug for 10 min. (B) Na^+ currents in the absence of the conditioning pre-pulse (same neuron as in A). Left panel: control currents. Note that at −30 mV the fast current was completely inactivated. Middle panel: currents after a 4-min perfusion with the local anesthetic. Inset: activation protocol. Right panel: currents after wash-out of the local anesthetic for 10 min.

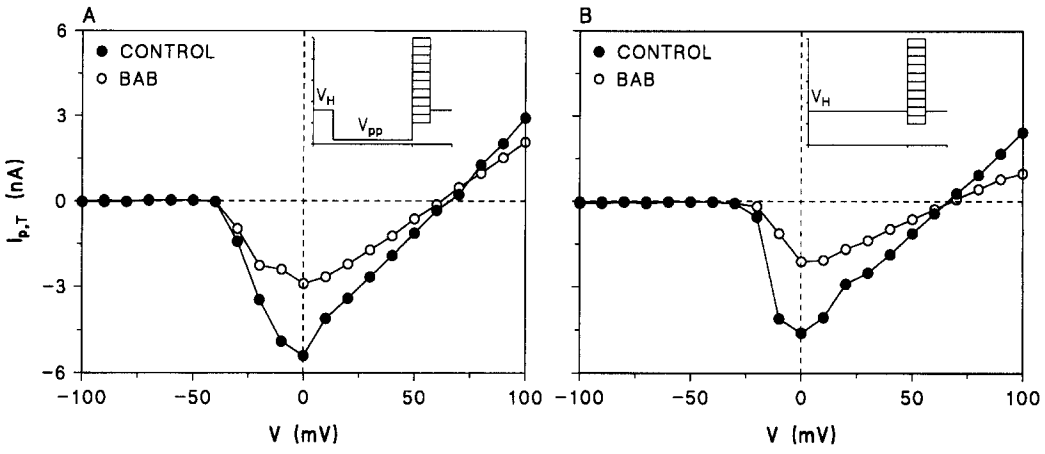

Fig. 3. Peak current-voltage relations, obtained from the currents depicted in Fig. 2. Closed and open symbols correspond to peak currents measured in the control and the drug-containing solution (BAB), respectively. (A) The peak current-voltage relation *with* a hyperpolarizing pre-pulse. Inset: activation protocol (not all test pulses shown). Regardless of whether the local anesthetic is present in the bathing medium, the sodium current activated at about −40 to −30 mV. The maximum inward amplitude was reached at 0 mV. The current reversed at +61 mV in the control and at +57 mV in the drug-containing solution, close to the calculated Na^+ Nernst potential of +60 mV. (B) The peak current-voltage relation *without* a hyperpolarizing pre-pulse. Inset: activation protocol (not all test pulses shown). The Na^+ current activated at about −20 to −10 mV in both control and drug-containing solution, and the maximum amplitude was reached around 0 mV. Obviously, the dominant slow current activated more steeply depending on voltage than the fast current. In the absence and presence of the local anesthetic, the Na^+ current reversed at +64 mV.

-21 ± 2 mV after wash-out of the toxin, were not statistically different, indicating a negligible contribution of fast Na^+ channels to the firing level.

Action potentials evoked in 9 out of 25 neurons, which were sensitive to *n*-butyl-*p*-aminobenzoate, could also be blocked by tetrodotoxin. This suggested that the local anesthetic can inhibit fast Na^+ channels. Moreover, the threshold voltage of 15 out of 40 neurons with *n*-butyl-*p*-aminobenzoate- and tetrodotoxin-resistant action potentials, amounting to -23 ± 1 mV in control solution was significantly ($P \leq 0.005$) raised both by the local anesthetic and the toxin to -16 ± 2 mV and reversed to -22 ± 1 mV after wash-out of the drugs. This indicated that fast Na^+ channels contributed to the firing threshold and that they were inhibited both by *n*-butyl-*p*-aminobenzoate and tetrodotoxin, in line with our previous results obtained with neurons cultured in a serum-free medium (Van den Berg et al., 1995a).

3.2. Sodium currents and membrane voltage

Fig. 2A shows typical inward and outward Na^+ currents at 5 membrane voltages (left panel). At −30 mV, only the fast Na^+ current was present whereas at 0 mV the slow Na^+ current started to dominate. At higher depolarizations, fast and slow currents coincided and became outward at +90 mV. The fast currents were completely and reversibly blocked by 200 nM tetrodotoxin. Fast Na^+ currents also could be reduced substantially by omitting the conditioning hyperpolarizing pre-pulse, so that the slow current dominated the responses at each test voltage (Fig. 2B, left panel).

The amplitude of the Na^+ current was diminished by the local anesthetic at all test potentials, irrespective of the conditioning pre-pulse (Fig. 2A,B). Evidently, both fast and slow Na^+ currents were reduced by *n*-butyl-*p*-aminobenzoate. The wash-out experiments demonstrated the reversible action of the drug and excluded artifacts that could be introduced by changing extracellular solutions or by rundown of the neuron (Fig. 2A,B, right panel). An example of peak current-voltage relations in the absence and presence of the local anesthetic, with or without the conditioning pre-pulse, is shown in Fig. 3A,B. In control solution, the Na^+ current reversed at $+63 \pm 3$ and $+59 \pm 4$ mV ($n = 11$), respectively, in the presence and absence of the pre-pulse, close to the calculated Na^+ Nernst potential of +60 mV. These values did not change statistically significantly during drug exposure, amounting to

Table 2
Peak Na^+ conductances g_p, g_p^o, $g_{p,F1}$, $g_{p,F2}$, $g_{p,F3}$, $g_{p,S1}$ and $g_{p,S2}$ at −10 mV in control, after 2–4 min of perfusion with the local anesthetic and after 5–10 min of washing-out

	Control (nS)	*n*	BAB (nS)	*n*	Wash-out (nS)	*n*
g_p	55±10	12	32±8 [a]	11	50±11	12
g_p^o	33±10	10	9±3 [a]	10	28±9	10
$g_{p,F1}$	12±4	9	12±3	9	10±3	8
$g_{p,F2}$	27±7	12	29±9	12	31±9	11
$g_{p,F3}$	29±16	7	7±6 [a]	7	33±17	5
$g_{p,S1}$	8±2	8	8±2	8	12±3	7
$g_{p,S2}$	36±8	8	4±2 [a]	8	35±9	7

The conductances were determined from $g_p = I_p/(V - V_{Na})$ (Hodgkin and Huxley, 1952). The quantities g_p and g_p^o are the conductances underlying the peak currents in the presence and in the absense of the hyperpolarizing prepulse. Data marked [a] are statistically significantly different from the control values. BAB, *n*-butyl-*p*-aminobenzoate.

61 ± 4 and 60 ± 4 mV, indicating that the local anesthetic did not affect the ionic selectivity of fast and slow Na^+ channels.

At test voltages of −30, 0 and +30 mV, we calculated the ratio of the peak current in the control to that in the presence of the local anesthetic. Obtained with pre-pulses, these ratios were 0.52 ± 0.05, 0.63 ± 0.03 and 0.68 ± 0.04 ($n = 11$), respectively, a statistically significant difference ($P \leq 0.02$). This suggests that the block by *n*-butyl-*p*-aminobenzoate is reduced at larger depolarizing steps. In the absence of the pre-pulse, the peak current ratios at the respective voltages were 0.10 ± 0.03, 0.41 ± 0.06 and 0.54 ± 0.08 ($n = 9$), indicating that the 'resting block' is increased by long-lasting depolarization. The ratios differ significantly ($P \leq 0.002$), again showing that the block by the local anesthetic becomes smaller at greater depolarizing steps. After wash-out, the peak currents were not statistically different from their values obtained under control conditions. Table 2 shows the conductances underlying the peak currents.

3.3. Inactivation of fast and slow Na^+ currents

To separate fast and slow Na^+ currents, we made use of the fact that the fast current was completely inactivated at

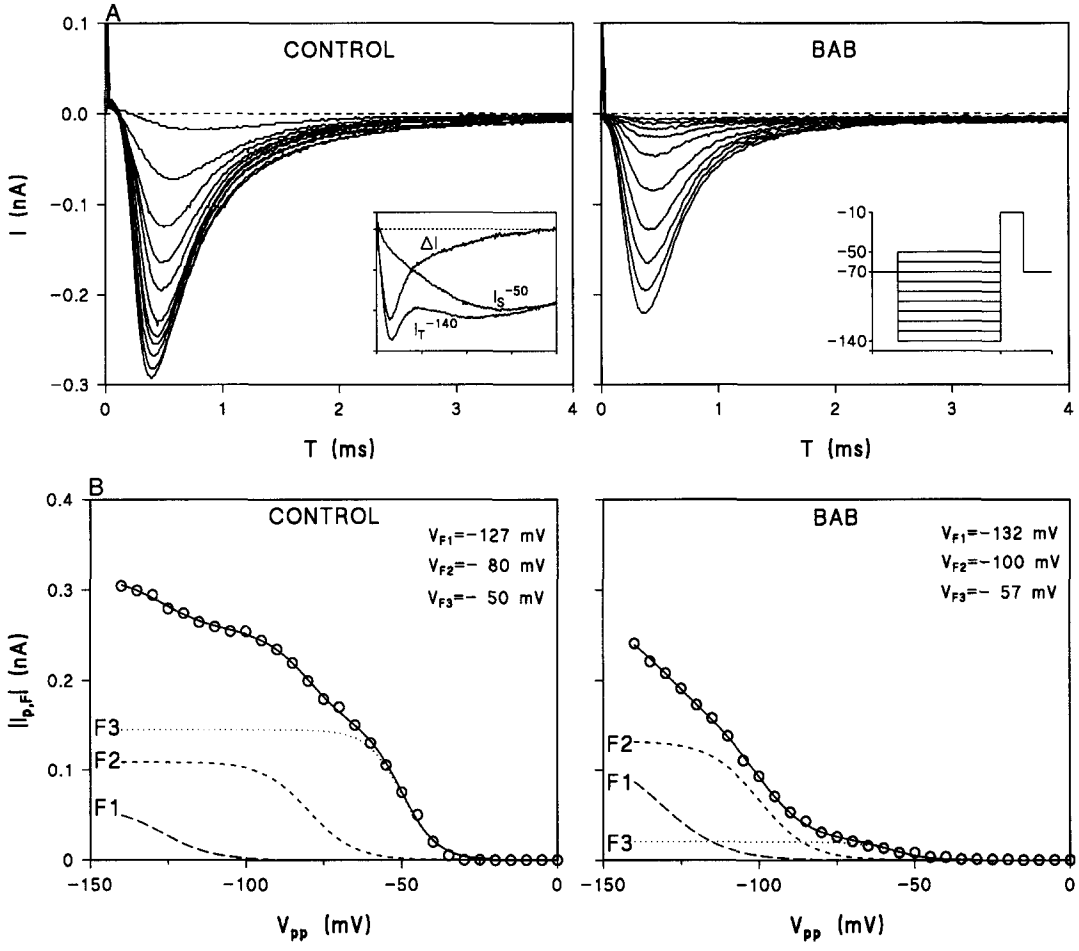

Fig. 4. Inactivation of fast Na^+ currents. (A) The Na^+ current was measured at the test voltage of −10 mV and was preceded by pulses varying from −140 to −40 mV. The neuron had a resting resistance of 503 MΩ. The series resistance amounted to 6.6 MΩ and was compensated by 60%. The membrane capacitance was 22 pF. For clarity, the currents corresponding to pre-pulses spaced by 10 mV instead of 5 mV are shown. Left panel: control currents. Inset: procedure for the separation of fast and slow currents (from a different neuron). Right panel: currents in the presence of the local anesthetic. Inset: voltage protocol (not all pulses shown). (B) Steady-state inactivation curve for fast Na^+ currents as shown in A. The circles represent the absolute value of the peak current in control (left panels) and in 100 μM *n*-butyl-*p*-aminobenzoate (right panels). The lines represent the fit of Eqn. 2 to these data. Note that, by applying Eqn. 2, the maximum peak current, being experimentally inaccessible, could be estimated (at the cost of accuracy). Curve-fitting yielded the following parameters in control: $\bar{I}_{F1} = 0.06 \pm 0.01$ nA, $\bar{I}_{F2} = 0.11 \pm 0.02$ nA, $\bar{I}_{F3} = 0.15 \pm 0.01$ nA, $V_{F1} = -127 \pm 3$ mV, $V_{F2} = -80 \pm 2$ mV, $V_{F3} = -50 \pm 1$ mV, $k_{F1} = 8.0$ mV (could not be obtained as a free parameter and was fixed to a value, at which the residual values were minimal), $k_{F2} = 7.4 \pm 1.3$ mV and $k_{F3} = 5.6 \pm 0.4$ mV. The parameters in the presence of the local anesthetic were: $\bar{I}_{F1} = 0.12 \pm 0.01$ nA, $\bar{I}_{F2} = 0.13 \pm 0.01$ nA, $\bar{I}_{F3} = 0.021 \pm 0.002$ nA, $V_{F1} = -132 \pm 3$ mV, $V_{F2} = -100 \pm 1$ mV, $V_{F3} = -57 \pm 2$ mV. The slope parameters were fixed to those obtained in control solution. Voltage errors due to residual series resistance were negligible with these small Na^+ currents. The increase of F_1 was present in a number of neurons and was a slow process, independent of the local anesthetic. Wash-out of the drug succeeded partially, but the midpoint potentials obtained were close to their control values.

pre-pulse potentials around −50 mV, where the slow current did not show any inactivation (Van den Berg et al., 1995a,b). By subtracting the (non-inactivated) slow current from the total Na^+ current, measured after pre-pulses more negative than −50 mV, we obtained the fast Na^+ current as a function of pre-pulse (Fig. 4A, left panel). In 9 out of 12 neurons, the fast current did not reach a maximum after pre-pulses up to −140 mV. This unusual inactivation is known to be present in newborn rats (Schwartz et al., 1990). In the presence of the local anesthetic, the degree of inactivation of the fast currents was increased (Fig. 4A, right panel).

Inactivation curves were obtained by plotting the amplitude of the peak current I_p as a function of pre-pulse potential V_{pp}. All curves were characterized by 2 or 3 declining limbs with increasing steepness. In all neurons, the relation between the peak of the fast current, $I_{p,F}$, and V_{pp} showed a characteristic bend around −100 mV, in 7 of 12 there was also a bend around −60 mV. A sum of 2 or 3 Boltzmann functions (cf., Van den Berg et al., 1995b)

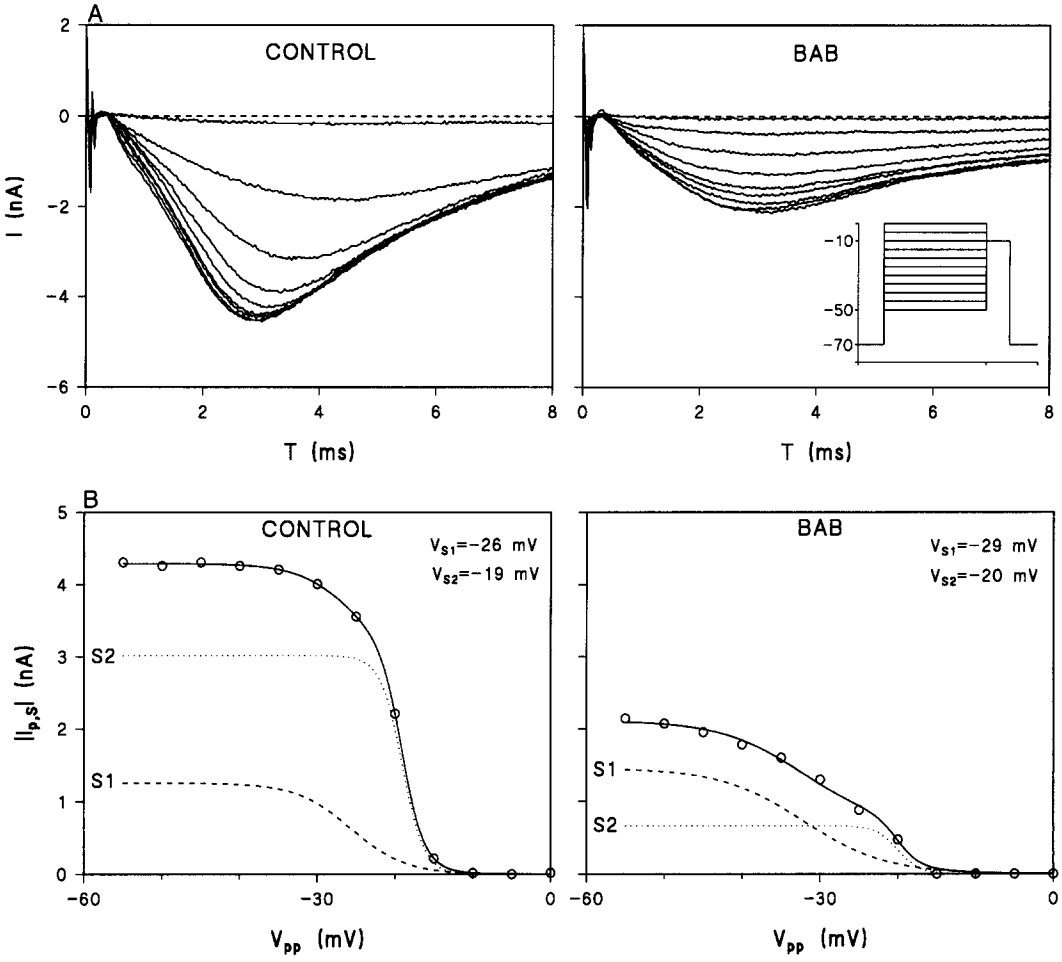

Fig. 5. Inactivation of slow Na^+ currents. (A) Slow Na^+ currents were measured at the test voltage of −10 mV preceded by pulses varying from −50 to 0 mV, spaced by 5 mV. Different neuron from the one in Fig. 4. The neuron had a resting resistance of 200 MΩ and a capacitance of 27.5 pF. The series resistance, amounting to 7.0 MΩ, was compensated by 80%. Left panel: control currents. For clarity, the (base-line) currents at pre-pulses of −5 and 0 mV are not shown. Right panel: currents in the presence of the local anesthetic. Inset: voltage protocol applied. (B) Steady-state inactivation curves of slow sodium currents as shown in A. The circles represent the absolute value of the amplitude of the peak current in control (left panel) and in 100 μM *n*-butyl-*p*-aminobenzoate (right panel). The lines represent the fit of Eqn. 3 to these data, yielding the following parameters in the control: $\bar{I}_{S1} = 1.26 \pm 0.38$ nA, $\bar{I}_{S2} = 3.0 \pm 0.4$ nA, $V_{S1} = -26 \pm 2$ mV, $V_{S2} = -19.1 \pm 0.1$ mV, $k_{S1} = 3.5 \pm 0.5$ mV and $k_{S2} = 1.4 \pm 0.2$ mV. The parameters in the presence of the drug were: $\bar{I}_{S1} = 1.7 \pm 0.1$ nA, $\bar{I}_{S2} = 0.41 \pm 0.13$ nA, $V_{S1} = -29 \pm 1$ mV, $V_{S2} = -20 \pm 1$ mV, $k_{S1} = 6.3 \pm 0.5$ mV and $k_{S2} = 1.4$ fixed to the value in the control. After wash-out of the drug, the parameters were similar to the control values with $\bar{I}_{S1} = 1.30 \pm 0.20$ nA and $\bar{I}_{S2} = 3.2 \pm 0.2$ nA. The control data points were also fitted by a single Boltzmann function. The best fit was obtained from the asymptotic information criterion (AIC) for the residual sum of squares (RSS), given by: N lnRSS + 2P with N the number of data points and P the number of free parameters (Akaike, 1981). The AIC amounted to −64 and −18 for Eqn. 3 (6 free parameters) and a single Boltzmann function (2 free parameters), respectively. Thus, the best fit, corresponding to the lowest value of AIC was obtained with Eqn. 3.

Table 3
Midpoint potentials and slopes of the inactivation curves for fast and slow Na^+ current components in the absence and presence of 100 μM *n*-butyl-*p*-aminobenzoate (BAB)

Parameter	Control (mV)	*n*	BAB (mV)	*n*	Wash-out (mV)	*n*
V_{F1}	−127±5	8	−134±3 [a]	8	−125±5	7
V_{F2}	−83±2	12	−104±1 [a]	12	−87±2 [a]	11 [b]
V_{F3}	−53±2	6	−59±2 [a]	4	−55±1	5
V_{S1}	−32±1	8	−29±2	8	−29±1	7
V_{S2}	−18±1	8	−16±1	6	−19±1	7
k_{F1}	9.3±1.5	9	9.2±1.3	9	9.6±1.4	8
k_{F2}	8.1±0.7	12	8.9±0.7	12	7.7±0.7	11
k_{F3}	4.6±0.6	6	6.8±1.5	4	5.7±1.2	5
k_{S1}	4.9±0.8	8	5.1±0.8	8	4.9±1.3	7
k_{S2}	2.7±0.3	8	2.8±0.7	6	2.5±0.3	7

The neurons were perfused with the drug-containing solution for 2–4 min, after which the wash-out lasted 5–10 min.
[a] Statistically significantly different from the control values.
[b] Significantly different from control ($P = 0.004$) due to either incomplete wash-out or spontaneous shift of the curve.

was necessary to give a reasonably accurate description of the inactivation curve for the fast current:

$$I_{p,F}(V_{pp}) = \frac{\overline{I_{F1}}}{(1+e^{(V_{pp}-V_{F1})/k_{F1}})} + \frac{\overline{I_{F2}}}{(1+e^{(V_{pp}-V_{F2})/k_{F2}})} + \frac{\overline{I_{F3}}}{(1+e^{(V_{pp}-V_{F3})/k_{F3}})} \quad (2)$$

where $\overline{I_{F1}}$, $\overline{I_{F2}}$ and $\overline{I_{F3}}$ are the maximum magnitudes of the respective Na^+ current components, V_{F1}, V_{F2} and V_{F3} their midpoint potentials (50% inactivation) and k_{F1}, $k_{F,2}$ and k_{F3} their slope factors. Of 12 neurons, 5 exhibited both F_1 and F_2 currents, 3 neurons had both F_2 and F_3 currents, while 4 neurons had all 3 fast current subtypes (Fig. 4B). Table 2 shows the peak conductances $g_{p,F1}$, $g_{p,F2}$ and $g_{p,F3}$ underlying the peaks of the fast current components at −10 mV. Their midpoint potentials and slopes are given in Table 3. After perfusion with the local anesthetic, the amplitudes of F_1 and F_2 currents were not significantly altered whereas the F_3 current was significantly reduced to 24% of the control value ($P < 0.0001$, cf., Table 2). This reduction was reversible within 10 min of wash-out. The midpoint potentials of F_1, F_2 and F_3 were all significantly shifted by the drug to hyperpolarizing voltages for 7, 21 and 6 mV, respectively ($P \leq 0.005$, Table 3). These shifts were largely reversible during wash-out. Only the inactivation curve for the F_2 current shifted up to −2 mV in the absence of the local anesthetic during a period of 10 min. Thus, the observed shifts can be completely attributed to the action of *n*-butyl-*p*-aminobenzoate. The slope factors were not statistically altered by the local anesthetic.

The inactivation of slow Na^+ currents is depicted in Fig. 5A. Here, there was a clear saturation of the peak current at levels around −50 mV. In the presence of the local anesthetic, the amplitude was reduced at all pre-pulse potentials. Similarly to Eqn. 2, the inactivation curve could be described by:

$$I_{p,S}(V_{pp}) = \frac{\overline{I_{S1}}}{(1+e^{(V_{pp}-V_{S1})/k_{S1}})} + \frac{\overline{I_{S2}}}{(1+e^{(V_{pp}-V_{S2})/k_{S2}})} \quad (3)$$

where $\overline{I_{S1}}$ and $\overline{I_{S2}}$ are the maximum peak amplitudes of components S_1 and S_2, V_{S1} and V_{S2} their midpoint potentials and k_{S1} and k_{S2} the slope factors (Fig. 5B). In 8 out of 12 neurons, both the S_1 and S_2 currents were present. The peak conductances $g_{p,S1}$ and $g_{p,S2}$ underlying the peaks of the slow current components at −10 mV are given in Table 2 and their midpoint potentials and slopes can be found in Table 3. In *n*-butyl-*p*-aminobenzoate-containing solutions, the S_1 current was not significantly changed in amplitude whereas the amplitude of S_2 was (reversibly) reduced to 11% of the control value ($P = 0.004$, cf., Table 2). The midpoint potentials and slopes of both slow components were not significantly altered by the drug (Table 3).

4. Discussion

Our findings indicated that the excitability of small neonatal dorsal root ganglion neurons was drastically reduced by dissolved *n*-butyl-*p*-aminobenzoate. In neurons cultured in our serum-enriched medium, 3 fast and 2 slow Na^+ current components were present. The local anesthetic differentially affected the various components of fast and slow Na^+ currents.

Resting membrane potentials of dorsal root ganglion neurons range from −70 to −50 mV with a mean of −60 mV (Wang et al., 1994). At this potential, the F_1 current is completely inactivated, F_2 by 94%, F_3 by 12%, whereas inactivation of S_1 and S_2 currents is completely absent. However, the midpoint potentials of the inactivation curves might have been shifted to negative potentials under our ionic conditions (Van den Berg et al., 1995a) and F_1 and F_2 currents may participate as well. Neglecting such contributions, during excitations from the resting potential only F_3, S_1 and S_2 currents play a role. Because S_1 is insensitive to the local anesthetic, reduction of excitability arises from the action of the drug on F_3 and S_2 currents. Tetrodotoxin-sensitive action potentials can only originate from the F_3 current, and their block by the local anesthetic in 23% of the neurons, is caused by block and inactivation of this current component. Also, the increase of the firing threshold by both the local anesthetic and tetrodotoxin in 37% of the neurons reflects effects on the F_3 current. Since this component occurred in ≈ 60% of the neurons under voltage clamp, there is reasonable agreement with our findings under current clamp conditions. Tetrodotoxin-resistant action potentials, which could be blocked by the local anesthetic in 40% of the current-clamped neurons,

can only arise from S_2 currents. This percentage of block was lower than the 67% of voltage-clamped neurons exhibiting the S_2 current, presumably through the firing of action potentials arising from S_1 currents. This current is also responsible for the tetrodotoxin- and *n*-butyl-*p*-aminobenzoate-resistant action potentials in 37% of the neurons. Since the amplitude of S_1 is much smaller than that of S_2, these observations may seem unexpected, but differences in activation voltage and kinetics may favour the role of the S_1 current. More information on this issue is necessary.

Our results are important in relation to the differential analgesic effect of *n*-butyl-*p*-aminobenzoate. In vivo, the spinal root nerve fibres in the epidural space are the main target tissue for the local anesthetic (Korsten et al., 1991). These fibres probably contain different proportions of fast and slow current components. If the distribution of current components as measured in neuron somata resembles that in axons, the S_2 current is dominant in pain-mediating C-fibres (Table 2). These fibres will be blocked by the local anesthetic, while other fibres (e.g., those with a dominating S_1 current) remain unaffected. Differential nerve block may also result from varying contributions of the F_3 current. In neurons with a large F_3 current, fast action potentials may still be generated after a 24% block whereas in neurons with a relatively small F_3 contribution such action potentials will be blocked or firing thresholds raised. We note that increased thresholds might attenuate the propagation of action potentials in vivo, resulting in nerve block (Van den Berg et al., 1994). At present, we cannot rule out the interesting possibility that the length of exposure is an important factor in differential nerve block (cf., Fink, 1989).

Several components of fast and slow Na^+ currents have been found in newborn rat dorsal root ganglion neurons. Omri and Meiri (1990) distinguished fast, intermediate and slow Na^+ currents, with inactivation midpoint potentials of -70, -29 and -21 mV, respectively. On the basis of these values, their fast current is a combination of F_2 and F_3 currents whereas their intermediate and slow currents correspond to our S_1 and S_2 currents, respectively. Schwartz et al. (1990) separated the Na^+ currents into a fast newborn, a fast adult and a slow component, with midpoint potentials of -139, -75 and -24 mV, respectively. The fast newborn current is, thus, similar to F_1 whereas the fast adult current corresponds to F_2 and F_3 currents. Finally, their slow current type corresponds to our S_2 current. Different Na^+ currents have also been found in adult rat dorsal root ganglion neurons (Caffrey et al., 1992).

Fast and slow Na^+ currents reflect the existence of distinct Na^+ channels (Akopian et al., 1996). It is tempting to speculate that distinct subtypes of fast and slow Na^+ channels underly the fast and slow Na^+ current components. Binding of etidocaine (200 μM) to the local anesthetic receptor site on transmembrane segment S6 (domain IV) near the pore of rat brain IIA Na^+ channels, shifted the inactivation curve by -24 mV (Ragsdale et al., 1994). On the other hand, external application of antibodies directed against the C_1^+ region of segments S4 shifted the voltage dependence of the fast adult current inactivation by -26 mV (Schwartz et al., 1990). Therefore, *n*-butyl-*p*-aminobenzoate molecules may bind to one of these inactivation-related sites of the channels underlying the F_2 current (-21 mV shift). The relatively small shift of the inactivation of F_1 (-7 mV) and of F_3 (-6 mV) may reflect a structural difference between these channels and F_2 channels or binding to another inactivation-related site. Binding of *n*-butyl-*p*-aminobenzoate to the conduction-related part of the Na^+ channel (S5–S6) may explain the block of F_3 channels. Such a block may also occur in S_2 channels, where the inactivation-related site is either missing or inaccessible. The smaller block at larger step depolarizations was most pronounced when the fast currents were inactivated. This voltage-dependent reduction of block may originate from the relief of the local anesthetic from S_2 channels during short depolarizing pulses.

Comparison with our previous study on the local anesthetic (Van den Berg et al., 1995a) showed a number of differences. The block of 'slow' action potentials (tetrodotoxin-resistant) by 100 μM *n*-butyl-*p*-aminobenzoate was not observed in that study, due to the absence of S_2 currents. Moreover, these neurons also lacked the fast currents, F_1 and F_3. The midpoint potentials of the single fast and slow currents in these experiments were -88 and -28 mV (± 2 mV), respectively, and, thus, correspond to the F_2 and S_1 components. The local anesthetic shifted the inactivation of the fast current -16 mV, without affecting the slow current (Van den Berg et al., 1995a), in agreement with the present findings for F_2 and S_1 currents. Since the use of serum is the only difference between this and the previous study, our results suggest that expression of Na^+ current components depends on culture conditions. Such a dependence was shown by Omri and Meiri (1990), who found that neurons exhibited solely the intermediate current in the absence of (β) nerve growth factor whereas in its presence in addition to the intermediate current both fast and and slow currents were present.

The Na^+ channels, underlying the various currents that completely inactivate after some time, must exist in at least 3 states: closed, open and inactivated (cf., Hille, 1992). We do not know which of these transitions is influenced by the local anesthetic. Measurement of the time course of development of inactivation (current decay) and of recovery from inactivation may help to partition the local anesthetic effect between increased rate of development of inactivation and a decrease in the rate of recovery (cf., Van den Berg et al., 1993). However, both decay of and recovery from inactivation reflect the kinetic properties of fast and slow currents. Therefore, such an analysis is only useful if one current component can be isolated, allowing analyses to discriminate between a modulated or guarded receptor for the local anesthetic (cf., Chernoff and Strichartz, 1990).

Nevertheless, our finding of differential Na^+ channel 'block' is important in the search for the mechanism of selective nerve fiber actions.

Acknowledgements

This work was supported by a grant from Abbott Laboratories (Hospital Products Division, Abbott Park, IL, USA). We thank Drs. T. Louis (University of Minnesota, MN, USA) and P.C. Molenaar (Laboratory of Physiology, Leiden, The Netherlands) for critical reading of this manuscript.

References

Akaike, H., 1981, Modern development of statistical methods, in: Trends and Progress in System Identification, Vol. 1, ed. P. Eykhoff (Pergamon, Oxford) p. 169.

Akopian, A., L. Sivilotti and J.N. Wood, 1996, A tetrodotoxin-resistant voltage-gated sodium channel expressed by sensory neurons, Nature 379, 257.

Baccaglini, P.I. and P.G. Hogan, 1983, Some rat sensory neurons in culture express characteristics of differentiated pain sensory cells, Proc. Natl. Acad. Sci. USA 80, 594.

Caffrey, J.M., D.L. Eng, J.A. Black, S.G. Waxman and J.D. Kocsis, 1992, Three types of sodium channels in adult rat dorsal root ganglion neurons, Brain Res. 592, 283.

Chernoff, D.M. and G.R. Strichartz, 1990, Kinetics of local anesthetic inhibition of neuronal sodium currents. pH and hydrophobicity dependence, Biophys. J. 58, 69.

Fink, B.R., 1989, Mechanisms of differential axial blockade in epidural and subarachnoid anesthesia, Anesthesiology 70, 851.

Hamill, O.P., A. Marty, E. Neher, B. Sakmann and F.J. Sigworth, 1981, Improved patch-clamp techniques for high resolution current recording from cells and cell-free membrane patches, Pflügers Arch. 391, 85.

Harper, A.A. and S.N. Lawson, 1985, Conduction velocity is related to morphological cell type in rat dorsal root ganglion neurons, J. Physiol. 359, 31.

Hille, B., 1992, Ionic Channels of Excitable Membranes (Sinauer Associates, Sunderland, MA) p. 485.

Hodgkin, A.L. and A.F. Huxley, 1952, A quantitative description of membrane current and its applications to conduction and excitation in nerve, J. Physiol. 117, 500.

Korsten, H.H.M., E.W. Ackerman, R.J.E. Grouls, A.A.J. Van Zundert, W.F. Boon, F. Bal, M.A. Crommelin, J.G. Ribot, F. Hoefsloot and J.L. Slooff, 1991, Long-lasting epidural sensory blockade by *n*-butyl-*p*-aminobenzoate in the terminally ill intractable cancer pain patient, Anesthesiology 75, 950.

Omri, G. and H. Meiri, 1990, Characterization of sodium currents in mammalian sensory neurons cultured in serum-free defined medium with and without NGF, J. Membr. Biol. 115, 13.

Ragsdale, D.S., J.C. McPhee, T. Scheuer and W.A. Catterall, 1994, Molecular determinants of state-dependent block of Na^+ channels by local anesthetics, Science 265, 1724.

Roy, M.L. and T. Narahashi, 1992, Differential properties of tetrodotoxin-sensitive and tetrodotoxin-resistant sodium channels in rat dorsal root ganglion neurons, J. Neurosci. 12, 2104.

Schwartz, A., Y. Palti and H. Meiri, 1990, Structural and developmental differences between three types of Na channels in dorsal root ganglion cells of newborn rats, J. Membr. Biol. 116, 117.

Shulman, M., 1987, Treatment of cancer pain with epidural butyl-aminobenzoate suspension, Reg. Anesth. 12, 1.

Van den Berg, R.J., P. Kok and R.A. Voskuyl, 1993, Valproate and sodium currents in cultured hippocampal neurons, Exp. Brain Res. 93, 279.

Van den Berg, R.J., C.A.A. Versluys, A. De Vos and R.A. Voskuyl, 1994, Nerve fibre size related block of action currents by phenytoin in mammalian nerve, Epilepsia 35, 1279.

Van den Berg, R.J., P.F. Van Soest, Z. Wang, R.J.E. Grouls and H.H.M. Korsten, 1995a, The local anesthetic *n*-butyl-*p*-aminobenzoate selectively affects inactivation of fast sodium currents in cultured rat sensory neurons, Anesthesiology 82, 1463.

Van den Berg, R.J., Z. Wang, R.J.E. Grouls and H.H.M. Korsten, 1995b, Fast and slow sodium currents in cultured dorsal root ganglion neurons, Eur. J. Neurosci. 8 (Suppl.), 147.

Wang, Z., R.J. Van den Berg and D.L. Ypey, 1994, Resting membrane potentials and excitability at different regions of rat dorsal root ganglion neurons in culture, Neuroscience 60, 245.

Wood, J.N., J. Winter, I.F. James, H.P. Rong, J. Teats and S. Bean, 1988, Capsaicin-induced ion fluxes in dorsal root ganglion cells in culture, J. Neurosci. 8, 3208.